A Review on Computational Fluid Dynamics Simulations of Industrial Amine Absorber Columns for CO_2 Capture

Mohammad Jamali[1], Ahmad Azari[1],*

Abstract

CO_2 emission is an important environmental issue leading to global climate change, notably an increase in global temperatures; therefore, it is so imperative to reduce CO_2 emissions to the atmosphere. Absorption columns using amine-based solutions are a promising approach for CO_2 removal from industrial gas streams. Many modeling and simulation research have been performed on CO_2 absorption columns in which computational fluid dynamics (CFD) strategy is very appropriate and well-known. As CFD modeling and simulation is a fast-developing method, the most recent review papers do not include the core research in this field of study. In this study, numerical simulations of CO_2 absorption columns using CFD strategy have been carried out applying various types of amine-based solutions. Furthermore, the effect of various types of packing mesh generation on the absorption columns' efficiency was studied. Investigation of synergetic influence such as application of various nanoparticles in different amine-based solutionsand activators, double diameter packed bed absorption columns with different packings, rotating packed columns with double diameter are proposed for future studies.

Keywords: Amine absorber columns, Computational fluid dynamics, CO_2 capture, Simulation & Modeling, Structured packing

Received: April 26, 2022; *revised:* July 14, 2022; *accepted:* October 26, 2022

DOI: 10.1002/cben.202200018

1 Introduction

Manufacturing, commercial and power plants are major producers of greenhouse gases in the atmosphere. Emissions of greenhouse gases, especially CO_2, followed by global warming, have a devastating effect on the environment [1–5]. On the other hand, CO_2 removal is an important step in industrial processing activities such as oil refining, ammonia synthesis, natural gas refining, coal gasification, and hydrogen manufacturing. Acidic gases such as CO_2 and H_2S cause human poisoning, catalyst poisoning and corrosion of materials [2, 3, 6, 7]. For this reason, carbon capture and storage (CCS) have been the subject of many researches so far.

CO_2 removal is performed by separation processes such as absorption, adsorption, membrane and cryogenic processes [1, 8–12]. The most prominent and widely used method of these methods is CO_2 adsorption with liquid solvents [12].

Solution absorption is done in a column with opposite flows of liquid and gas. The absorption columns have a packing bed to create a suitable contact surface between the gas containing CO_2 and the liquid. The amount of CO_2 absorption and mass transfer depends on the distribution of liquid flow on the packings [13–15]. Structured packings are widely used in absorption, distillation, scrubbing and extraction columns, and these offer a highly effective area per unit volume [16–18].

The use of amines for CO_2 capture is one of the oldest and most well-known CO_2 capture techniques that has been well established in many industries and can be used on a large scale [19–21]. CO_2 absorption by amine solution and use of structure packings for direct contact of gas and liquid cause excellent mass transfer efficiency and low pressure drop, good wettability, ease of installation and a high capacity [2, 18, 20, 22-28]. Monoethanolamine (MEA) and diethanolamine (DEA) are suitable ethanolamine solutions for adsorption due to their low volatility, thermal stability, high reactivity, and low capital cost [29]. Tab. 1 provides a summary of amine solvents in chemical absorption processes.

In an experimental study, Penttila et al. [30] investigated the Henry's law constant of CO_2 in aqueous binary and ternary solutions of MEA, DEA, DIPA, MDEA, and AMP.in 1997, Hikita et al. [29] studied the kinetics of CO_2 reaction with MEA, DEA, and TEA. Afkhamipour and Mofarahi [5] investigated the performance of CO_2 absorption using amine-based solvents in high and low pressure in structured packings. Mofarahi et al. [31] designed a CO_2 absorption plant for recovery of CO_2 from the flue gases of gas turbines with amine

[1] Mohammad Jamali,
Dr. Ahmad Azari https://orcid.org/0000-0001-8878-947X
Department of Chemical Engineering, Faculty of Petroleum, Gas and Petrochemical Engineering, Persian Gulf University, Bushehr, 75169-13817, Iran.
E-Mail: Azari.Ahmad@pgu.ac.ir, Azari.Ahmad@gmail.com

Table 1. Summary of amine solvents in chemical absorption processes [7].

Solvent	Advantage	Disadvantage
Monoethanolamine (MEA)	High reactivity and fast absorption rate, which allows absorption to take place in a shorter column.	Limited CO_2 loading capacity due to formation of rather stable carbamates.
	Low absorption of hydrocarbon	Degradation through irreversible side reactions with CO_2 and O_2.
		Operational issue such as solvent loss, foaming, fouling, increased viscosity and corrosion.
Diethanolamine (DEA)	High reactivity and fast absorption rate.	Limited CO_2 loading capacity.
	The carbamate of DEA is not as stable as the carbamate of MEA.	Proneness to a certain extent of corrosion and solvent degradation.
Methyldiethanolamine (MDEA)	Higher CO_2 loading compared to MEA and DEA due to formation of the bicarbonate ion instead of carbamates.	Slow absorption kinetics with CO_2.
	Low heat of reaction with the acid gases, which leads to lower energy requirements for regeneration.	
	Lower solvent degradation rate compared to MEA and DEA.	
	Not corrosive to carbon steel.	
Diisopropanolamine (DIPA)	Less corrosive than MEA or DEA solutions.	Moderate rates of reaction with CO_2 and are prone to a certain extent of corrosion and solvent degradation.
	Less heat required in the regeneration of the solution.	
		Greater selectivity for H_2S over CO_2.
2-Amino-2-methyl-1-propanol (AMP)	Higher CO_2 loading capacity compared to MEA.	Lower absorption rate compared to MEA
	Relatively low energy consumption required for solvent regeneration.	
	Less corrosion.	
	Higher degradation resistance.	

solvents such as, DEA, DGA, MDEA, and MEA. In another project, Salkuyeh and Mofarahi [32] compared MEA and DGA performance for CO_2 capture under different operational conditions. Nuchitprasittichai and Cremaschi [33], analyzed the impact of different amine absorbents and their concentrations, the absorber and stripper column heights and the operating conditions on the cost of CO_2 recovery plants for post-combustion CO2 removal. Talkhan et al. [34] studied absorption of CO_2 in aqueous blends of MDEA and arginine. Costa et al. [35, 36], experimentally investigated different piperazine (PZ)/MDEA mixtures and compared their performance with that of single reagents. They showed that small quantities of PZ added to MDEA aqueous solutions were sufficient to obtain a significant improvement in the kinetics of the process. Tan et al. [7] studied factors affecting the efficiency of absorption packing columns including physical properties of solvents, CO_2 partial pressure and total system pressure, gas flow rate, liquid flow rate, absorbent concentration, and liquid temperature. Kale et al. [37] modeled the reactive absorption of CO_2 using MEA. In their work, two different types of structured packing, Sulzer BX and Sulzer MellapakTM 250.Y, were employed. The model predicted the experimental profiles of the temperature and concentration of CO_2 in the liquid phase with an accuracy of ± 8 %. Kvamsdal et al. [38] presented a dynamic modeling and simulation of a CO_2 absorber columns for post-combustion CO_2 capture.

Today, computational fluid dynamics (CFD) is widely used to simulate CO_2 capture. CFD as a powerful, reliable, cost saving and suitable technique for the design and optimization of processes that can help study the performance and hydrodynamic behavior of packed bed columns and structure packings in various dimensions that cannot be done in experiments [27, 28, 39–48].

Some studies on the modeling and simulation of CO_2 capture based on software such as Aspen Plus using amine solvents have been reported, and, in some studies, CFD and other software have been coupled [49–56]. Also, modeling and simulation of CO_2 absorption using hollow fiber membranes (HFM) with amine solution with computational fluid dynamics has been done by researchers [57–59]. CO_2 absorption using CFD, however, has rarely been done, especially in industrial amine absorber columns.

Aristopour and Abbasian [60] used CFD to investigate the performance of absorption columns with several solvents at different temperatures. Aroonwilas et al. [2] presented a mechanistic model that can predict mass-transfer performance and

provides an insight into dynamic behavior within structured packings used for CO_2 absorption. Asendrych et al. [61] and Niegodajew and Asendrych [62] Used a CFD model to investigate CO_2 capture by monoethanolamine in an absorber column. In their studies, Eulerian model was employed to resolve the flow in a random packed bed. Kim et al. [22] applied a porous media Eulerian CFD model to an amine absorber packed M250X for capturing CO_2 from the post-combustion flue gas. They investigated the effect of the four modification factors of the Ergun coefficients on liquid holdup and pressure drop. Pham et al. [20] extended the gas-liquid Eulerian porous media CFD model to consider mass transfer and chemical reaction in an amine absorber with a Mellapak 500.X structured-packing. Model parameters of the porous resistance and momentum exchange were adjusted to fit experimental data. In another study, Pham et al. [63] investigated the effects of ship motion on acid gas removal performance in an amine absorber with a Mellapak 500.X structured packing. Pan et al. [15] developed a validated device-scale CFD model that could predict quantitatively both hydrodynamic and CO_2 capture efficiency for an amine-based solvent absorber column with a random Pall ring packing. Gbadago et al. [64] used CFD to investigate a multi-packed bed amine absorption column with interbed liquid distributors on an AMT SP-350Y structured packing by dividing the packed column into five beds. They used a Eulerian multiphase model for the study. Also, the hydrodynamic properties in one, two, and five packed bed MEA columns with interbed liquid distributors were investigated. Fu et al. [65] studied the influence of random packed column parameters (including packing types, solvent properties, and operating conditions) on the liquid holdup and interfacial area using CFD. Tab. 2 lists some representative CFD simulations of industrial absorber columns for CO_2 capture.

Isoz et al. [43, 67] used a CFD model to study the gas flow through different types of commercial structured packings (Mellapak 250.X, 250.Y, 350.Y, and 500.Y) and investigated the effects of packing geometry. Sun et al. [68] studied the hydrodynamic performance of two structured packings, Mellapak 250Y and Montzpak B1–500, for gas-liquid flow. Xue et al. [69] designed, investigated, and compared a wire gauze packing with initial packings to improve hydrodynamic performance. The novel wire gauze structured packing PACK-1300Y with a high specific surface area was investigate by Hassanvand et al. [70]. In another study, Manh et al. [71] studied a novel wire gauze structured packing, PACK-860, and the main features of PACK-860, such as height equivalent to a theoretical plate (HETP) and evaluated the pressure drop. Basha et al. [72] modeled multiphase flow distribution in a packed-bed absorber with structured packing Mellapak 250Y. Experimental and CFD studies by Yu et al. [46] were done on the effects of surface texture on liquid thickness, wetted area and mass transfer in Mellapak 125.X structured packings. In these studies, a CFD model was validated using experimental data, and then it is used to investigate the effects of packing geometry. Kawas et al. [73] presented accurate models for evaluating the hydrodynamic and separation behavior of an innovative packing structure called Tetra Spline (TS). Amini et al. [74] carried out an experimental and numerical investigation of mass transfer efficiency in a new wire gauze with a high-capacity structured packing. They investigated various operational conditions to assess the optimal parameters such as the HETP of PACK-2100 in the distillation column. Tab. 3 shows some studies on structured packings using CFD.

Haroun et al. [78] used CFD to investigate the liquid holdup and mass transfer as time-varying functions on structured packing beds. They used the volume of fluid (VOF) approach

Table 2. Some representative CFD simulations of industrial absorber columns for CO_2 capture.

Reference	Year	Contribution
Asendrych et al. [61]	2013	CO_2 capture by MEA
Aristopour and Abbasian [60]	2014	Performance of absorption columns with several solvents at different temperatures
Pham et al. [20]	2015	Mass transfer and chemical reaction in an amine absorber with a Mellapak 500.X structured-packing
Pham et al. [63]	2015	Effects of ship motion on acid gas removal performance in an amine absorber with a Mellapak 500.X structured packing
Niegodajew and Asendrych [62]	2016	CO_2 capture by MEA
Kim et al. [22]	2016	Application of a porous media Eulerian CFD model to an amine absorber packed M250X for capturing CO_2
Pan et al. [15]	2018	Quantitative prediction of hydrodynamic and CO_2 capture efficiency for an amine-based solvent absorber column with a random Pall ring packing
Gbadago et al. [64]	2020	Multi-packed bed amine absorption columns with interbed liquid distributors on an AMT SP-350Y structured packing divided into five beds
Uwitonze et al. [66]	2021	the impact of offshore operating conditions and that of divided wall column shape with 3D CFD model
Fu et al. [65]	2022	The influence of random packed column parameters on the liquid holdup and interfacial area

Table 3. Some studies on structured packings using CFD.

Reference	Year	Structured packing
Pham et al. [20]	2015	Mellapak 500.X
Pham et al. [63]	2015	Mellapak 500.X
Kim et al. [22]	2016	Mellapak 250.X
Isoz et al. [43]	2017	Mellapak 250.X and Mellapak 250.Y
Isoz et al. [67]	2018	Mellapak 250.X, 250.Y, 350.Y, and 500.Y
Yu et al. [46]	2018	Mellapak 125.X
Amini et al. [74]	2019	PACK-2100
Gbadago et al. [64]	2020	AMT SP-350.Y
Manh et al.[71]	2020	PACK-860
Basha et al. [72]	2020	Mellapak 250.Y
Sun et al. [68]	2021	Mellapak 250.Y and Montzpak B1–500
Xue et al [69]	2021	Wire gauze
Hassanvand et al. [70]	2021	PACK-1300Y
Kawas et al. [73]	2021	Tetra Spline (TS)
Uwitonze et al. [66]	2021	MellaPak 500.Y
Amini et al. [75]	2021	Dixon ring
Al-Maqaleh et al. [76]	2022	Tetraspline
Kang et al. [77]	2022	Raschig ring and a helical ring

to simulate a two-dimensional amine absorbent with structured packages. The results show that liquid velocity and geometry affected the liquid film and surface mass transfer. In another project, Haroun et al. [16] studied the effective of the surface area and liquid (MEA) holdup on packings using CFD. In their work, they showed that CFD is a suitable tool to study the performance characteristics of packings. They also showed that CFD could be used to determine the fluid flow behavior, interfacial surface, and liquid holdup. Sebastia-Saez et al. [79] developed a three-dimensional CFD model on a small scale for hydrodynamic and physical mass transfer in structured packing elements. The results of the model were validated with theory and reported experimental data. For hydrodynamics, the liquid film thickness and wetted area were calculated, whereas for mass transfer, the Sherwood number and concentrations of the dissolved species were predicted. The CFD results reasonably matched the experimental and theoretical data. Kang et al [28, 80, 81] studied hydrodynamic behavior in random packings using CFD simulations. They showed that CFD simulations can obtain reasonable predictions of hydrodynamic behavior of packings, and that the inclusion of microstructures into a packing element will improve its hydrodynamic properties. Cooke [82] modeled the reactive absorption in gas-liquid flows in structured packings that led to the development of the enhanced surface film (ESF) model. The ESF approach was chemically able to simulate enhanced absorption of gaseous species into thin liquid films. Dong et al. [83] determined the liquid mass-transfer coefficients for the absorption of CO_2 in alkaline aqueous solutions in structured packings using CFD. Also, Yang et al. [84] modeled the hydrodynamic characteristics of multiphase counter-current flows in a structured packed bed using CFD. Singh et al. [85–88] investigated the effect of absorbent properties, contact angle, and dynamic contact angle (DCA) on the effective surface area and wet structured packing area in several studies. The Kapitza number, which depends only on the physical properties of absorbents, was proposed for surface area analysis.

To the best of our knowledge, up to now no comprehensive review papers have been published on the modeling and simulation of CO_2 absorption columns with amine-based solutions. Therefore, in the present work, a great effort has been made for gathering and reviewing numerous papers on the CFD simulation and modeling of CO_2 absorption columns. The governing equations, different simulation models, mass transfer efficiency and hydrodynamic properties, including pressure drops and liquid holdup parameters of different researches will be considered and their advantages and disadvantages will be discussed to show novel ways for future studies. Fig. 1 shows the most important findings of the paper.

2 Governing Equations

The CFD simulation of industrial amine absorbers use the Eulerian multiphase model in which the gas and liquid phases are treated as interpenetrating continua. Mass and momentum transfers between the gas and liquid phases are implemented and closed by closure equations. The fluid flow is assumed to be continuous, incompressible and isothermal [20, 22]. Fig. 2 shows the overview of the governing equations.

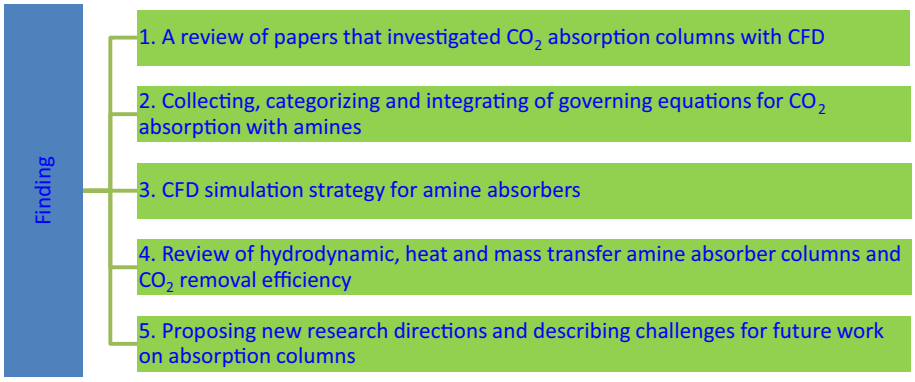

Figure 1. Most important findings of the paper

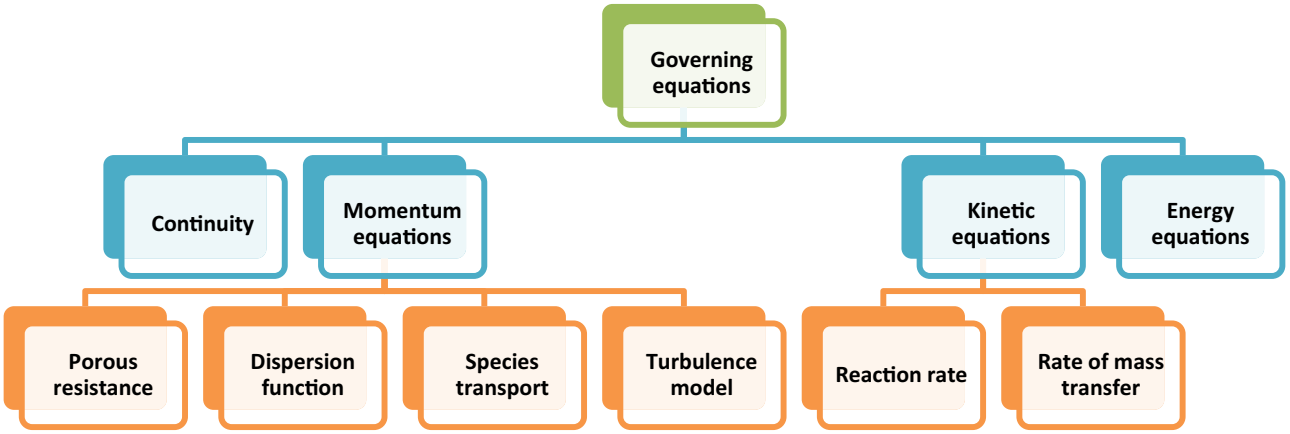

Figure 2. Overview of governing equations.

2.1 Continuity

The volume fractions for all the phases sum up to unity:

$$\sum_{i=1}^{n} \alpha_i = 1 \tag{1}$$

The mass continuity equation for the two-phase system is written as:

$$\frac{\partial}{\partial t}\alpha_i \rho_i + \nabla\left(\alpha_i \rho_i \vec{u}_i\right) = R_i \tag{2}$$

where α_i is the i-th phase volume fraction, ρ_i is the i-th phase density, u_i is the velocity vector of the i-th phase, and R_i is the total rate of mass transfer in the i-th phase.

2.2 Momentum Equation

The momentum equation for the i-th phase of the Eulerian model has the following form:

$$\begin{aligned}&\frac{\partial}{\partial t}\left(\alpha_i \rho_i \vec{u}_i\right) + \nabla\left(\alpha_i \rho_i \vec{u}_i \vec{u}_i\right) = \nabla\left(\mu_i \alpha_i \nabla \vec{u}_i\right)\\ &- \alpha_i \nabla p + \alpha_i \rho_i \vec{g} + \vec{F}_{D,i}\\ &+ \vec{F}_{VM,i} \dot{M}_i \vec{u}_i + \vec{S}_i + \vec{F}_{disp}\end{aligned} \tag{3}$$

where, μ is the viscosity, p is the pressure, g is the gravity vector, F_D is the drag force, F_{VM} is the virtual mass force, $\dot{M}$ is the contribution of mass transfer, S_i is the porous resistance, and F_{disp} is the liquid dispersion force.

2.2.1 Porous Resistance

In the porous region, which is the most important amine absorber column section, the porous resistance is:

$$\vec{S}_i = \frac{\mu_i}{\sigma_i}\vec{u}_i + C_i \frac{1}{2}\rho_i \left|\vec{u}_i\right| \vec{u}_i \tag{4}$$

Here, s_i the permeability of the porous media, and C_i is the inertial resistance. On the right hand side, the first term is the viscous loss term and the second one represents the inertial momentum loss. The values of these coefficients were determined in an experimental way for the air flow in a dry column and were believed to be nearly constant for the low volume fraction levels [61]. The porous resistance force in each phase is expressed by the generalized Ergun correlation in packed beds [89, 90]. Tab. 4 shows porous media model parameters and the model parameters of mass-transfer of one amine (MEA).

Table 4. Porous media model parameters and model parameters of mass-transfer of MEA.

Parameters	Value
Ergun coefficients [–]	$E_1 = 160$, $E_2 = 0.16$
Modification factors of Ergun coefficients [–]	$a = 1.9$, $b = 1.37$, $c = 0.17$, $d = 1.16$
Surface tension of MEA solution [N m^{-1}]	$\sigma = 0.0623$
Diffusivities of gas and liquid [m^{2}s^{-1}]	$D_g = 2.8 \times 10^{-7}$, $D_l = 2.88 \times 10^{-9}$

2.2.2 Dispersion Function

A dispersion function to liquid distribution in a structured packing has been proposed [20, 22, 64, 89, 91]. The proposed model is defined as:

$$\vec{F}_{disp,g} = \alpha_g K_{s,g} \vec{u}_{D,g} + \varepsilon K\left(\vec{u}_{D,g} - \vec{u}_{D,l}\right) \tag{5}$$

$$\vec{F}_{disp,l} = \alpha_l K_{s,l} \vec{u}_{D,l} - \varepsilon K\left(\vec{u}_{D,g} - \vec{u}_{D,l}\right) \tag{6}$$

where $K_{S,g}$ is the gas-solid drag, $K_{S,l}$ is the liquid-solid drag, K is the drag coefficient of momentum exchange, $u_{D,i}$ is the drift

velocity, and $u_{D,r}$ is the relative drift velocity between phases. The $K_{S,g}$ and $K_{S,l}$ are defined as:

$$K_{S,g} = \frac{aE_1}{36}\frac{a_s^2}{\varepsilon}\mu_g + \frac{bE_2}{6}\frac{a_s\alpha_g\rho_g}{\varepsilon}\left|\vec{u}_g\right| \tag{7}$$

$$K_{S,l} = \frac{aE_1}{36}\frac{\varepsilon a_s^2}{\alpha_l^2}\mu_l + \frac{bE_2}{6}\frac{\varepsilon a_s\rho_l}{\alpha_l}\left|\vec{u}_l\right| \tag{8}$$

where E_1 and E_2 are the Ergun coefficients, a_S [m^2m^{-3}] is the specific surface area of the packing, and a and b are the modification factors for the Ergun coefficient [24]. The drift velocities are defined as:

$$\vec{u}_{D,g} = -\frac{f_{spread}\left|\frac{\vec{u}_g}{\alpha_g}\right|}{\alpha_g}\vec{\nabla}\alpha_g \tag{9}$$

$$\vec{u}_{D,l} = -\frac{f_{spread}\left|\vec{u}_l\right|}{\alpha_l}\vec{\nabla}\alpha_l \tag{10}$$

where f_{spread} is the spreading factor with a unit of the length and was obtained from the liquid flow distribution interpreted with a convection-diffusion equation of q_l (liquid load or liquid volumetric flux, $m^3m^{-2}h^{-1}$) [89]:

$$\frac{\partial q_l}{\partial z} = f_{spread}\frac{1}{r}\frac{\partial}{\partial r}\left(r\frac{\partial q_r}{\partial r}\right) \tag{11}$$

where q_r is the radial liquid load.

Dimensions of the gas dispersion force ($F_{disp,g}$) are much smaller than those of the liquid dispersion force ($F_{disp,l}$).

2.2.3 Species Transport

The absorption of CO_2 into amine occurs in a two-step mechanism. First, CO_2 is transferred from the gas phase into the liquid phase, and then, the liquid CO_2 is transferred into the amine solution. By combining the two steps, an overall species transport equation can be written as [64]:

$$\frac{\partial}{\partial t}\left(\alpha_i\rho_i Y_{i,j}\right) + \nabla\left(\alpha_i\rho_i\vec{u}_i Y_{i,j}\right) - \nabla\left(\alpha_i\rho_i D_{i,j}\nabla Y_{i,j}\right) = \dot{m}_{i,j} + \alpha_i R_{i,j} \tag{12}$$

Here, $Y_{i,j}$ is the mass fraction of specie j in phase i, $R_{i,j}$ is the mass transfer rate between gas and liquid, $\dot{m}_{i,j}$ is the homogeneous chemical reaction and D is the diffusion coefficient. The transport equation is solved for only $N_s - 1$ species with the total mass fraction of species in each phase equal to unity:

$$\sum_{j=1}^{n} Y_{i,j} = 1 \tag{13}$$

2.2.4 Turbulence Model

The flow field in CO_2 absorber column is usually considered to be turbulent. The turbulent modelling is based on the standard $k-\varepsilon$ and RNG $k-\varepsilon$ models [85–87, 92, 93]. The turbulent viscosity is written as:

$$\frac{\partial}{\partial t}(\rho k) = \nabla\left(\rho\frac{\mu_t}{\sigma_k}\nabla k\right) + G_k + \frac{2}{3}\rho\left(\nabla\vec{u}\right)k - \rho\varepsilon + S_k \tag{14}$$

Here, ∇k is the effective diffusion coefficient for the turbulent kinetic energy, σ_k is an empirical constant, G_k is the rate of production of k, S_k is the source term, and μ_t is the turbulent viscosity written as:

$$\mu_t = C_\mu\frac{k^2}{\varepsilon} \tag{15}$$

Here, C_μ is the Eddy–viscosity coefficient, and the dissipation is written as:

$$\frac{\partial}{\partial t}(\rho\varepsilon) = \nabla\left(\rho\frac{\mu_t}{\sigma_\varepsilon}\nabla\varepsilon\right) + \frac{C_1G_k\varepsilon}{k} - \frac{2}{3}C_1\rho\left(\nabla\vec{u}\right)\varepsilon - C_2\rho\frac{\varepsilon^2}{k} + S_\varepsilon \tag{16}$$

where C1, C2, and σ_ε are empirical constants.

2.3 Kinetic Equations

2.3.1 Reaction Rate

The reaction between CO_2 and amines has been studied extensively [29, 94–103]. Caplow [104] proposed the reaction based on the zwitterion mechanism which was presented by Danckwerts [105] as follows:

$$2RNH_2 + CO_2 \longrightarrow RNH_3^+ + RNHCOO^- \quad \text{Primary and secondary} \tag{17}$$

$$R_1R_2R_3N + CO_2 + H_2O \longrightarrow R_1R_2R_3NH^+ + HCO_3^- \quad \text{Tertiary} \tag{18}$$

and:

$$R = k_2[CO_2][\text{Amine}] \tag{19}$$

Where, for example, for MEA [106]:

$$\log(k_2) = 10.99 - \frac{2152}{T} \tag{20}$$

Here, T is the temperature (kelvin), and k_2 is the second-order reaction rate constant.

Experimental kinetic data of carbon dioxide with alkanolamines have been provided by some researchers [29, 95, 107, 108].

2.3.2 Rate of Mass Transfer

The mass transfer rate has been used for modeling with the two-film theory. The mass transfer coefficients in liquid and gas phases are defined as [109, 110]:

$$\frac{1}{K_l} = \frac{1}{Ek_l} + \frac{1}{Hk_g} \tag{21}$$

Where k_l and k_g are the mass transfer coefficients in the liquid and gas film, respectively, K_l is the overall liquid mass transfer coefficient, E is the enhancement factor, and H is Henry's constant. The liquid-side resistance ($1/k_l$) in the CO_2-amine system has the most effect on the overall mass transfer resistance ($1/K_l$) [102, 111, 112]. Therefore, the overall mass transfer coefficient can be written as follows:

$$K_x \cong E k_x \tag{22}$$

The enhancement factor (E) is expressed as a function of the amine concentration [109, 113]. The overall rate of mass transfer can then be defined as:

$$\dot{M} = E k_l a_e \rho_i \left(Y_{i,j}{}^{\star} - Y_{i,j}\right) \tag{23}$$

Here, $Y_{i,j}{}^{\star}$ is the interfacial mass transfer, and a_e is the interfacial area. The interfacial mass transfer ($Y_{i,j}{}^{\star}$) and the liquid-side mass transfer coefficient (k_l) are calculated using Henry's constant and the Sherwood number, respectively:

$$Y_{i,j}{}^{\star} = H_{i,j} Y_{i,j} \frac{\rho_d}{\rho_c} \tag{24}$$

$$k_l = \frac{sh_{i,j} D_{i,j}}{d_{i,j}} \tag{25}$$

And a_e can be written as [24]:

$$\frac{a_e}{a_s} = 1.34 \left[\frac{\rho_l}{\sigma} g^{\frac{1}{3}} \left(\frac{Q}{L_p} \right)^{\frac{4}{3}} \right]^{0.116} \tag{26}$$

$$Q = 5.1189 A h_L^{2.854} \tag{27}$$

Here, σ [N m^{-1}] is the surface tension of the amine solution, Q [m^{3}s^{-1}] is the liquid flow rate, L_p [m] signifies the wetted perimeter, A [m^2] is the cross-sectional area of column, and h_l is the liquid holdup. Where Eq. (27) is regressed from air-water experimental data [114] for liquid holdup (h_l) versus liquid load (q_l) in packing. a_e/a_s defined as the wetting-area fraction (f_e) that is the ratio of the effective contacting area between the gas and liquid phases to the specific surface area, that causes in connecting hydrodynamics and mass transfer. Since the effective interfacial area (a_e) cannot be directly captured because of an interpenetrating behavior of the multiphase flow in the Eulerian approach, it is considered as a function inspired. When the physical properties are assumed to be constant, f_e is expressed as a function of the liquid holdup [24].

2.4 Energy Equations

The energy conservation for CO_2 and amine solution is written as [64, 115]:

$$\begin{aligned} &\frac{\partial}{\partial t}\left(\alpha_i \rho_i (H_\alpha + K_\alpha)_i\right) \\ &+ \nabla\left(\left(\alpha_i \rho_i \vec{u}_i (H_a + K_a)_i\right) - \nabla\left(\alpha_i \alpha_i^{-\text{eff}} \nabla H_{\alpha i}\right)\right) = \\ &\alpha_i \frac{\partial \bar{p}}{\partial t} + \rho_i \vec{g}\,\vec{u}_i + \alpha_i \dot{Q}_R + \dot{Q}_{KE} + \dot{Q}_{TD} \end{aligned} \tag{28}$$

where, H_a is the enthalpy of the i-th phase, K_a is the kinetic energy, $\alpha_i^{-\text{eff}}$ is the effective thermal diffusivity, $\dot{Q}_R$ is the rate of heat change due to reaction, $\dot{Q}_{KE}$ is the kinetic energy, and $\dot{Q}_{TD}$ is the rate of heat change due to the temperature difference.

$$\dot{Q}_{KE} = m_{\alpha \ln}(K_{\alpha^{-1}} - K_\alpha) \tag{29}$$

$$\dot{Q}_{TD} = h_{j\alpha}(T_f - T_\alpha) \tag{30}$$

Here, $h_{j\alpha}$ is the heat transfer coefficient of the j-th specie in the i-th phase, T_f is the interface temperature, and T_α is the phase temperature.

3 CFD Simulation Strategy for Amine Absorbers

3.1 Mesh Generation

The choice of mesh size significantly affects the accuracy and numerical stability of CFD simulations. However, extremely fine or high-resolution meshes come at the expense of computational time. As a result, compromises need to be made between accuracy and computational cost. Near-wall treatment of the columns are considered with very fine meshes closest to the walls to fully capture flow effects and turbulence at the walls [64]. Fig. 3 shows the mesh details of the absorber column domain with one liquid distributor. The geometry of the liquid distributor is relatively more complex than that of the porous zone, and its structure consists of a non-conformal mesh. The upper and lower sides at the interface between the liquid distributor and the porous zone have a different mesh structure, and fine meshes are needed in the upper side because, in this area, gas and liquid collide, and this needs to be shown well for optimum column design. Some researchers [20, 22, 64] used hexahedral mesh structures to represent the liquid distributor, and a relatively coarse mesh structure was used in the porous zone just below the distributor.

3.2 Models

The main numerical models for the multiphase flow in both liquid and gas phases are assumed as a continuum fluid and momentum, and continuity equations are solved for both phases [20]. Two common approaches to the simulation of multiphase flows inside packed columns are Eulerian and the volume of fluid (VOF) models [22, 48, 116–124]. The differences between these two methods are as follows [125]:

– The VOF focuses on modelling the liquid flow locally on the surface of the packing and is suitable for micro-scale local

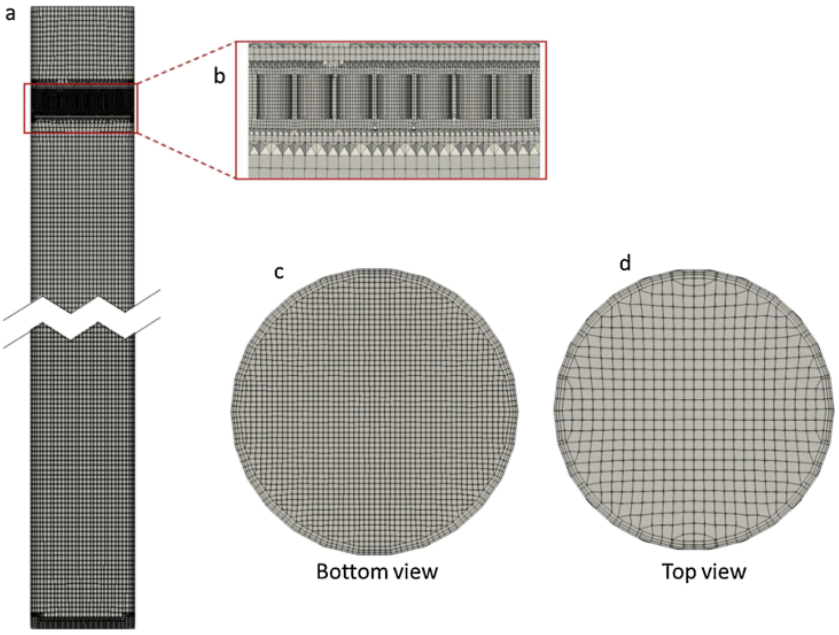

Figure 3. Mesh details of the absorber column domain with one liquid distributor [64].

simulations. The VOF model requires a very small grid size to capture the droplets and film, so it is not suitable for simulating 3D or large pilot scales due to simulation time limitations. However, the Eulerian method can simulate the liquid flow through the whole bed with the appropriate mesh size and with low requirement for computer resources.

- The VOF method requires a transient simulation, which takes a much longer time, while the Eulerian method can carry out the steady-state simulation and save much more computational time.
- The VOF method can achieve a clear liquid surface to the air and does not need a special model to obtain the interfacial area whereas the Eulerian method gives a liquid fraction in a unit volume and cannot give the interfacial area through the simulation.
- The VOF method treats the gas and liquid as one phase in the momentum equation, and the only force considered for the interaction between the gas and liquid is the surface tension. In contrast, the Eulerian method treats the gas and liquid as individual phases. The method needs the porous media model to describe the flow resistance between the gas or liquid and the packing, the gas-liquid drag model and the interfacial area model to estimate the surface between the gas and liquid.

Nevertheless, Amini and Esfahany [126] described these two models in their work and Ngo and Lim [127] reviewed the volume of fluid (VOF) and Eulerian multiphase CFD models for the gas-liquid phase. Pham et al. [128] presented a Eulerian-Eulerian porous media CFD model of amine absorbers for MEA-CO_2 system.

4 Hydrodynamics, Heat and Mass Transfer

4.1 Pressure Drop and Liquid Holdup

The pressure drop and liquid holdup are key determinants in CO_2 removal efficiency and overall absorber performance [61, 126, 129]. Zakeri et al. [129] experimentally investigated the pressure drop and liquid holdup in absorber columns. Amini et al. [130] carried out experimental and numerical simulations of pressure drop in high-capacity structured packings for determining the correlation between the pressure drop and structural dimensions of the structured packing. Also, Amini et al. [126] collected some significant researches on the application of the CFD approach to the investigation of hydrodynamics in structured packings. Fernandes et al. [131] showed that CFD can be used to calculate the pressure drop for both laminar and turbulent flow conditions. Using CFD, Hosseini et al. [42] studied pressure drop in structured packings. They proposed a simple method for evaluating the liquid holdup. Also, Sebastia-Saez et al. [108] used CFD to study pressure drop and liquid holdup in structured packing materials. The interfacial effective area and liquid holdup in structured packing geometries were investigated by Haroun et al. [16] using CFD. Owens et al. [23] developed a gas-phase Eulerian CFD simulation in a 3D real geometry model to calculate the dry gas pressure drop in packing columns. By comparing the pressure drop values calculated using simulation with the experimental ones, it was observed that there was a good agreement between the two sets of results. Qi et al. [132] investigated he mechanism and optimization of the dry pressure drop within a novel structured packing by CFD. Mazarei Sotoodeh et al [47] developed a model to evaluate the pressure drop of catalytic structured packings MCSP-11 and 12. According to their CFD results, the pressure drop in closed channels was higher than that in open channels. Tang et al. [133] examined experimental and modeling development of pressure drop in concurrent gas-liquid columns with a tridimensional rotational flow sieve tray. Singh et al. [86] simulated multiphase flows using CFD in a representative elementary unit (REU) of packed columns and its hydrodynamics on a microscale. Results show that the interfacial area and liquid holdup decreased with increase in the contact angle. Qiao et al. [134] conducted systematic experiments to measure the pressure drop of a gas flow through six sieve plate packings. The results indicated that the geometric characteristics of the packing had complicated effects on the pressure drop. Hendry et al. [135] studied the pressure drop and flooding in rotating packed beds. Some researchers [114, 136–139] presented empirical models for liquid holdup in packed columns to predict the values of normalization liquid holdup. Recently, Xue et al. [69] investigated and designed a novel type of structured wire

gauze packing and compared it with initial packings to improve hydrodynamic performance. They used a new multiscale CFD method for the first time to calculate the pressure drop of a structured wire gauze packing. Macfarlan et al. [140] studied the geometry of structured packings using CFD to determine its impact on the liquid-phase hydrodynamics such as the liquid holdup, liquid flow angle, and the Fanning friction factor. The hydrodynamic CFD predictions demonstrated excellent agreement with the experimental holdup data, with a six percent average deviation.

The type and velocity of the gas and operating conditions are the parameters that affect the pressure drop [126]. By increasing the gas flow rate, the liquid holdup increases until flooding occurs [141]. The pressure drop occurs in the porous zone, and the pressure change outside this zone is negligible. This indicates the importance of the flow resistance term appearing in this region. Just below the porous zone, the liquid content dramatically drops as a result of its acceleration, due to reduced flow resistance [142].

The number of meshes do not highly influence the CFD results, such as pressure drop and liquid holdup. In general, an unstable behavior of the liquid holdup is observed on the coarse mesh from the medium and fine meshes. Fig. 4 shows the results of a mesh independence test on coarse, medium and fine meshes from three studies.

Although the pressure drop is proportional to the height of the porous media, factors such as the liquid holdup also affect the pressure drop [143]. Gbadago et al. [64] Simulated three towers with different configurations (type A (single bed), type B (double bed), and type C (5-beds)) using CFD, as shown in Fig. 5.

Type A has the lowest pressure drop, and types B and C come second and third, respectively. Different liquid holdup values were observed for the three different absorber types. Type A showed the least liquid holdup, followed by type B, and then type C. Fig. 6 shows the column gauge pressure along the absorber height for the three configurations.

Process engineers can provide insights into possible installation points or locations for the installation of side streams used to control the temperature and efficiency of CO_2 absorbents by shedding light on the distribution of fluid and holdup in different parts of the absorber column.

4.2 Heat and Mass Transfer

A variety of turbulence models have been used to perform numerical simulations of heat and mass transfer for CO_2 capture. Fernandes et al. [131] modeled the packing geometry with a very detailed CFD and showed that CFD could be used to characterize the complex single and multiphase flows inside the packed beds and to evaluate the influence of the shape and geometry of the packing on the hydrodynamics, mass and heat transfer rates for both laminar and turbulent flow conditions. Results were seen to agree well with the experimental data in the literature. Macfarlan et al. [144] used CDF to study the methods applicable in turbulent flow conditions and interphase mass transfer methodologies used in structured packings. Chu et al. [145] studied turbulent models for CO_2 capture using

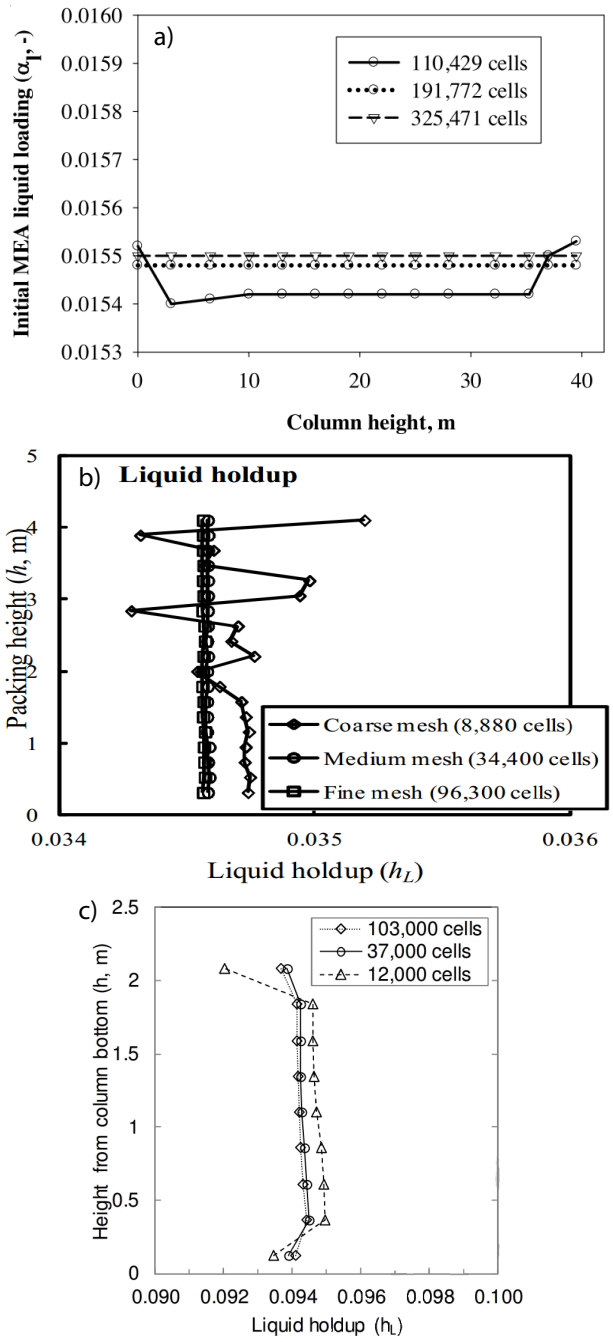

Figure 4. Results of a mesh independence test on coarse, medium and fine meshes from a) [64], b) [22], and c) [20].

MEA aqueous solutions in coal-fired power plants by modeling and optimizing absorbing columns. In another project, Chu et al. [146] investigated the turbulent models of the mass and heat transfer of MEA regeneration processes in packed columns. Three-dimensional CFD simulations in the representative elementary units of a structured packing were conducted by Singh et al. [87]. The SST $k-\omega$ turbulence model (a two-equation eddy-viscosity model) was used in turbulent flow simulations. In modelling the packing geometry, the dry pres-

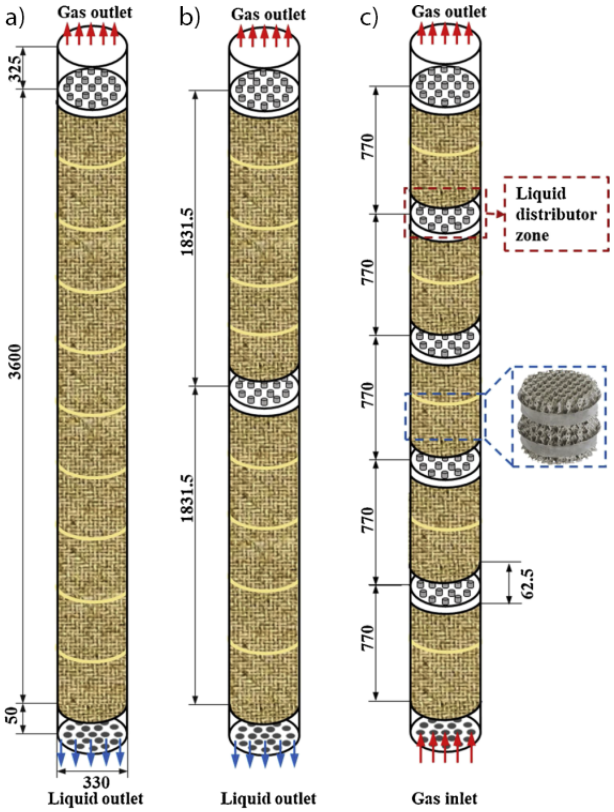

Figure 5. Geometry of MEA absorbers; a) Type A with one bed and one liquid distributor, b) Type B with two beds and liquid distributors, and c) Type C with five beds and liquid distributors [64].

sure drop was calculated for both laminar and turbulent flow conditions. Results showed good agreement with the experimental data in the literature. Fu et al. [147] experimentally analyzed the mass and heat transfer of CO_2 absorption using hybrid solvent MEA–MeOH in an absorption column. Yu et al. [148] identified the multi-ion effects on the phase flow, as well as mass and heat transfer in amine absorption of CO_2. They showed that the multi-ion in the aqueous CO_2-amine system inevitably influenced the mass and heat transfer and fluid flow, which were characterized by the turbulent diffusivity for mass transfer, turbulent thermal diffusivity for heat transfer and turbulent viscosity. The mass transfer performance of CO_2 absorption by amine solutions in packed columns has also been investigated by some researchers [5, 149]. Tab. 5 shows some studies on turbulent models using CFD.

Table 5. Some studies on turbulent models using CFD.

Reference	Year	Description
Fernandes et al. [131]	2008	Mass and heat transfer rates for both laminar and turbulent flow conditions
Fu et al. [147]	2015	Experimental analysis of mass and heat transfer of CO_2 absorption using hybrid solvent MEA–MeOH
Chu et al. [145]	2016	Turbulent models for CO_2 capture using MEA aqueous solutions
Yu et al. [148]	2017	Effects of the phase flow, mass and heat transfer on amine absorption of CO_2
singh et al. [87]	2018	The use of SST k-ω turbulence model in turbulent flow simulations
Chu et al. [146]	2021	Turbulent models of mass and heat transfer of MEA regeneration process in packed columns
Macfarlan et al. [144]	2022	Methods applicable in turbulent flow conditions and interphase mass transfer methodologies

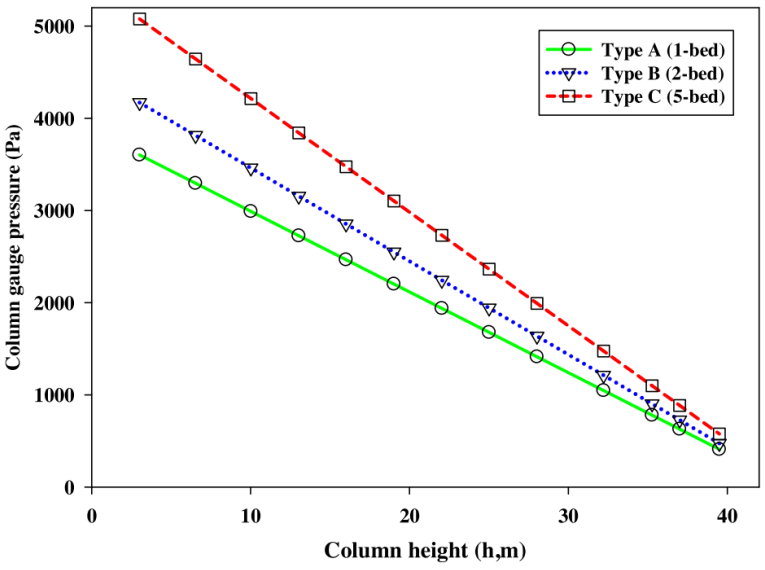

Figure 6. Column gauge pressure along the absorber height for the three configurations [64].

5 CO_2 Removal Efficiency

The equation of the overall CO_2 absorption efficiency is as follows:

$$CO_2 \text{ removal efficiency} = \frac{X_{CO_2}^{inlet} - X_{CO_2}^{outlet}}{X_{CO_2}^{inlet}} \times 100\% \quad (31)$$

where X_{CO_2} is the average mass fraction of CO_2 in the column's cross-section.

The packed bed height equivalent to a theoretical plate (HETP) determines the mass transfer performance of packed columns in distillation processes. In order to evaluate the mass transfer efficiency of a packed bed column, researchers often use the equivalent height to estimate a theoretical plate (HETP) in the distillation process. HETP is an empirical but very practical factor that enables designers to estimate the packed bed height based on the number of theoretical stages. The mass transfer efficiency for two-phase flows in a structured packed column was simulated using CFD by Haghshenas Fard et al. [41].

Amini et al. [74] experimentally and numerically studied mass transfer efficiency in a new wire gauze with a high-capacity structured packing. They investigated various operational conditions to assess the optimal parameters such as the HETP of PACK-2100 in the distillation column. The real geometry and model of structure PACK-2100 are shown in Fig. 7. Fig. 8 presents the contours of the mass fraction of CH_4O in the liquid phase within the constructed PACK-2100 on two vertical and three horizontal sections at F-factor = 0.45 $m\,s^{-1}$ $(kg\,m^{-3})^{0.5}$. Fig. 8 shows the variation of the concentration along the axis of packing. Fig. 9 presents the experimental data and numerical simulation results of mass transfer efficiency of PACK-2100.

Macfarlan et al. [144] reviewed the various methods implemented with CFD to predict mass transfer in structured packings, including methods applicable in turbulent flow conditions.

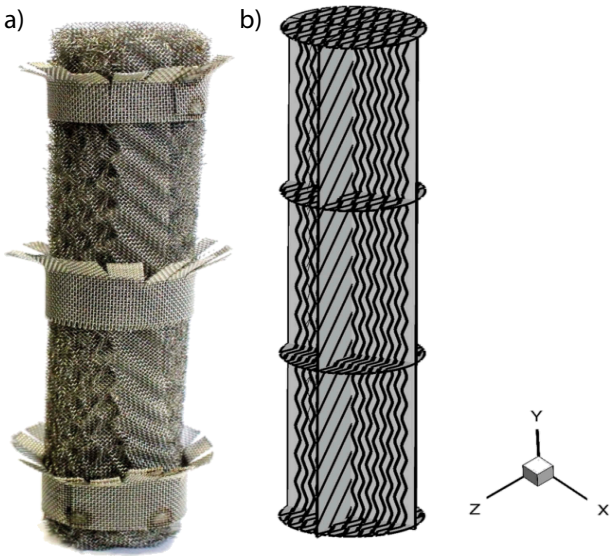

Figure 7. a) PACK-2100 [74] and b) computational domain [74].

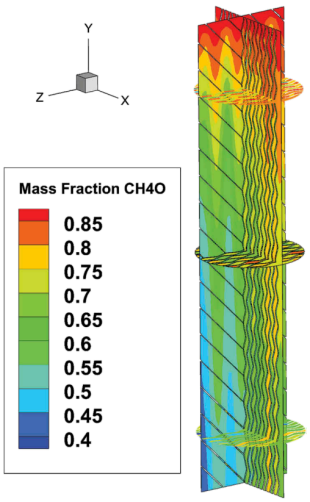

Figure 8. Methanol mass fraction profile in the liquid phase in PACK-2100 [74].

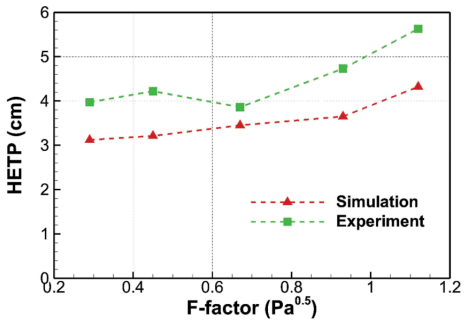

Figure 9. Comparison of experimental and simulated HETP for PACK-2100 [74].

6 Summary

CFD is an efficient and powerful tool that can explain the single and multi-phase behavior of fluids and economic design and simulation of processes. CFD simulations show an appropriate ability to study the performance and hydrodynamic behavior of packed bed columns and structured packings in various dimensions while showing good agreement with experimental data. This review presented a comprehensive research on the numerical CFD simulation of amine-based solutions in packed absorption columns. The effects of different factors, including governing equations, different simulation models, mass transfer efficiency and hydrodynamic properties, including pressure drop and liquid holdup, were evaluated based on the published literature. Furthermore, the capability of various numerical CFD approaches for simulating models considering their advantages and deficiencies were reported and the obtained results were compared. As far as suggestions for future studies are concerned, we recommend considering novel nanomaterials, including metal organic frameworks (MOFs), covalent organic frameworks (COFs) in amine solutions (nanofluids) and their combinations with conventional materials such as SiO_2, TiO_2, Fe_3O_4, combination of nano- and amine-

based solutions (nanofluids), double-diameter packed absorption columns with different packings, multi-diameter bubble columns, rotating packed columns with double diameters and different types of amine-based solutions such as a-MDEA (in which a refers to activator), DEA and TEA modified by suitable activators. Studying the synergetic effects of various fields, including magnetic, ultrasonic and other fields in combination with conventional methods are attractive fields which can improve the CO_2 absorption capacity. Finally, a great effort should be made in order to scale up the lab experiments for industrial purposes, for both economic and efficiency reasons.

Conflicts of Interest

The authors declare no conflict of interest.

Ahmad Azari is currently Associate Professor of Chemical Engineering at the Persian Gulf University and Director of the Applied Computational Fluid Dynamic Research Group. He teaches heat and mass transfer, computational fluid dynamic concepts, process modeling and simulation. His research interests focus on CFD simulation, process optimization, CO_2 separation, nanofluid heat and mass transfer, and industrial wastewater treatment for resource recovery and reuse in the Energy and Environment Research Center. He holds a B. Eng. degree in Chemical Engineering from Shiraz University (2006), an M.Sc. in Chemical Engineering from University of Tehran (2008), and a Ph.D. in Chemical Engineering from Amirkabir University of Technology (2012).

Mohammad Jamali received both his B.Sc. and M.Sc. in Chemical Engineering in 2014 and 2017, respectively from Persian Gulf University (PGU). He is presently a Ph.D. student in PGU, and his research interests are CO_2 capture, Computational Fluid Dynamics (CFD), amine solution thermodynamics, mass transfer, and modeling and simulation.

Symbols used

A	[m^2]	cross-sectional area of column
a	[–]	Ergun equation modification factor
a_e	[m^2m^{-3}]	interfacial area
a_s	[m^2m^{-3}]	specific surface area of the packing
b	[–]	Ergun equation modification parameter
C	[m^{-1}]	inertial resistance
C_μ	[–]	Eddy–viscosity coefficient
c	[–]	Ergun equation modification parameter
d	[–]	Ergun equation modification parameter
D	[m^2s^{-1}]	diffusion coefficient
E	[–]	enhancement factor
E_1	[–]	Ergun equation fitting parameter
E_2	[–]	Ergun equation fitting parameter
F_D	[$kg\,m^{-2}s^{-2}$]	drag force
F_{VM}	[$kg\,m^{-2}s^{-2}$]	virtual mass force
F_{disp}	[$kg\,m^{-2}s^{-2}$]	dispersion force
g	[m^2s^{-1}]	gravity
h	[–]	heat transfer coefficient
h_l	[m]	liquid holdup
H	[$Pa\,m^3kg^{-1}mol^{-1}$]	Henry's constant
H_α	[J]	enthalpy
K	[$kg\,m^{-3}s^{-1}$]	drag exchange coefficient
K_α	[J]	kinetic energy
K_l	[$m\,s^{-1}$]	overall liquid mass transfer coefficient
K_S	[$kg\,m^{-3}s^{-1}$]	phase-solid drag coefficient
k_2	[$kgmol\,m^{-3}s^{-1}$]	second-order reaction rate constant
k_g	[$kgmol\,Pa^{-1}m^{-2}s^{-1}$]	gas side mass transfer coefficient
k_l	[$m\,s^{-1}$]	liquid side mass transfer coefficient
L_p	[m]	wetted perimeter
M	[–]	contribution of mass transfer
N_s	[–]	number of species
p	[Pa]	pressure
Q	[m^3s^{-1}]	liquid flow rate
q_l	[$m^3m^{-2}h^{-1}$]	liquid load or liquid volumetric flux
q_r	[$m^3m^{-2}h^{-1}$]	radial liquid load
R	[$kg\,m^{-3}s^{-1}$]	rate of mass transfer
S	[$kg\,m^{-2}s^{-2}$]	porous resistance force
Sh	[–]	Sherwood number
t	[s]	Time
T	[K]	temperature
u	[$m\,s^{-1}$]	velocity
Y	[–]	species mass fraction

Greek letters

α	[–]	phase volume fraction
μ	[$kg\,m^{-1}s^{-}$]	viscosity
ε	[–]	bed porosity
ρ	[$kg\,m^{-3}$]	density

s	[–]	porous media permeability
σ	[N m^{-1}]	surface tension

Subscripts

disp	dispersed phase
c	continuous phase
g	gas phase
l	liquid phase
i,j	phases
r	relative

References

[1] M. Songolzadeh, M. Soleimani, M. Takht Ravanchi, R. Songolzadeh, *Sci. World J.* **2014**, *2014*, 828131. DOI: https://doi.org/10.1155/2014/828131

[2] A. Aroonwilas, A. Chakma, P. Tontiwachwuthikul, A. Veawab, *Chem. Eng. Sci.* **2003**, *58 (17)*, 4037–4053. DOI: https://doi.org/10.1016/S0009-2509(03)00315-4

[3] M. R. Rahimpour, M. Saidi, M. Baniadam, M. Parhoudeh, *J. Nat. Gas Sci. Eng.* **2013**, *15*, 127–137. DOI: https://doi.org/10.1016/j.jngse.2013.10.003

[4] I. Sreedhar, T. Nahar, A. Venugopal, B. Srinivas, *Renewable Sustainable Energy Rev.* **2017**, *76*, 1080–1107. DOI: https://doi.org/10.1016/j.rser.2017.03.109

[5] M. Afkhamipour, M. Mofarahi, *RSC Adv.* **2017**, *7 (29)*, 17857–17872. DOI: https://doi.org/10.1039/C7RA01352C

[6] Y. S. Choi, S. Nesic, S. Ling, *Electrochim. Acta* **2011**, *56 (4)*, 1752–1760. DOI: https://doi.org/10.1016/j.electacta.2010.08.049

[7] L. Tan, A. Shariff, K. Lau, M. Bustam, *J. Ind. Eng. Chem.* **2012**, *18 (6)*, 1874–1883. DOI: https://doi.org/10.1016/j.jiec.2012.05.013

[8] A. Lawal, M. Wang, P. Stephenson, G. Koumpouras, H. Yeung, *Fuel* **2010**, *89 (10)*, 2791–2801. DOI: https://doi.org/10.1016/j.fuel.2010.05.030

[9] B. P. Spigarelli, S. K. Kawatra, *J. CO2 Util.* **2013**, *1*, 69–87. DOI: https://doi.org/10.1016/j.jcou.2013.03.002

[10] A. Aroonwilas, P. Tontiwachwuthikul, *Chem. Eng. Sci.* **2000**, *55 (18)*, 3651–3663. DOI: https://doi.org/10.1016/S0009-2509(00)00035-X

[11] S. Hafeez, T. Safdar, E. Pallari, G. Manos, E. Aristodemou, Z. Zhang, S. Al-Salem, A. Constantinou, *Front. Chem. Sci. Eng.* **2021**, *15 (4)*, 720–754. DOI: https://doi.org/10.1007/s11705-020-1992-z

[12] J. Pires, F. Martins, M. Alvim-Ferraz, M. Simões, *Chem. Eng. Res. Des.* **2011**, *89 (9)*, 1446–1460. DOI: https://doi.org/10.1016/j.cherd.2011.01.028

[13] Z. Chen, D. Yates, J. K. Neathery, K. Liu, *Chem. Eng. Res. Des.* **2012**, *90 (3)*, 328–335. DOI: https://doi.org/10.1016/j.cherd.2011.07.024

[14] R. Notz, H. P. Mangalapally, H. Hasse, *Int. J. Greenhouse Gas Control* **2012**, *6*, 84–112. DOI: https://doi.org/10.1016/j.ijggc.2011.11.004

[15] W. Pan, J. Galvin, W. L. Huang, Z. Xu, X. Sun, Z. Fan, K. Liu, *Greenhouse Gases: Sci. Technol.* **2018**, *8 (3)*, 603–620. DOI: https://doi.org/10.1002/ghg.1770

[16] Y. Haroun, L. Raynal, P. Alix, *Chem. Eng. Res. Des.* **2014**, *92 (11)*, 2247–2254. DOI: https://doi.org/10.1016/j.cherd.2013.12.029

[17] A. Shilkin, E. Kenig, Z. Olujic, *AIChE J.* **2006**, *52 (9)*, 3055–3066. DOI: https://doi.org/10.1002/aic.10937

[18] N. Razi, O. Bolland, H. Svendsen, *Int. J. Greenhouse Gas Control* **2012**, *9*, 193–219. DOI: https://doi.org/10.1016/j.ijggc.2012.03.003

[19] N. S. Kwak, J. H. Lee, I. Y. Lee, K. R. Jang, J. G. Shim, *Energy* **2012**, *47 (1)*, 41–46. DOI: https://doi.org/10.1016/j.energy.2012.07.016

[20] D. A. Pham, Y. I. Lim, H. Jee, E. Ahn, Y. Jung, *Chem. Eng. Sci.* **2015**, *132*, 259–270. DOI: https://doi.org/10.1016/j.ces.2015.04.009

[21] Q. Zhuang, R. Pomalis, L. Zheng, B. Clements, *Energy Procedia* **2011**, *4*, 1459–1470. DOI: https://doi.org/10.1016/j.egypro.2011.02.012

[22] J. Kim, D. A. Pham, Y. I. Lim, *Comput. Chem. Eng.* **2016**, *88*, 39–49. DOI: https://doi.org/10.1016/j.compchemeng.2016.02.006

[23] S. A. Owens, M. R. Perkins, R. B. Eldridge, K. W. Schulz, R. A. Ketcham, *Ind. Eng. Chem. Res.* **2013**, *52 (5)*, 2032–2045. DOI: https://doi.org/10.1021/ie3016889

[24] R. E. Tsai, A. F. Seibert, R. B. Eldridge, G. T. Rochelle, *AIChE J.* **2011**, *57 (5)*, 1173–1184. DOI: https://doi.org/10.1002/aic.12345

[25] D. Beugre, S. Calvo, M. Crine, D. Toye, P. Marchot, *Chem. Eng. Sci.* **2011**, *66 (17)*, 3742–3752. DOI: https://doi.org/10.1016/j.ces.2011.02.049

[26] B. Sun, L. He, B. Liu, F. Gu, C. Liu, *AIChE J.* **2013**, *59 (8)*, 3119–3130. DOI: https://doi.org/10.1002/aic.14082

[27] B. Sun, T. Bhatelia, R. P. Utikar, G. M. Evans, V. K. Pareek, *Chem. Eng. Res. Des.* **2021**, *167*, 6–9. DOI: https://doi.org/10.1016/j.cep.2021.108533

[28] J. L. Kang, W. F. Chen, Y. C. Ciou, D. S. H. Wong, S. S. Jang, *Comput.-Aided Chem. Eng.* **2017**, *40*, 13–18. DOI: https://doi.org/10.1016/B978-0-444-63965-3.50004-0

[29] H. Hikita, S. Asai, H. Ishikawa, M. Honda, *Chem. Eng. J.* **1977**, *13 (1)*, 7–12. DOI: https://doi.org/10.1016/0300-9467(77)80002-6

[30] A. Penttilä, C. Dell'Era, P. Uusi-Kyyny, V. Alopaeus, *Fluid Phase Equilib.* **2011**, *311*, 59–66. DOI: https://doi.org/10.1016/j.fluid.2011.08.019

[31] M. Mofarahi, Y. Khojasteh, H. Khaledi, A. Farahnak, *Energy* **2008**, *33 (8)*, 1311–1319. DOI: https://doi.org/10.1016/j.energy.2008.02.013

[32] Y. K. Salkuyeh, M. Mofarahi, *Int. J. Energy Res.* **2012**, *36 (2)*, 259–268. DOI: https://doi.org/10.1002/er.1812

[33] A. Nuchitprasittichai, S. Cremaschi, *Comput. Chem. Eng.* **2011**, *35 (8)*, 1521–1531. DOI: https://doi.org/10.1016/j.compchemeng.2011.03.016

[34] A. G. Talkhan, A. Benamor, M. Nasser, M. H. El-Naas, S. A. El-Tayeb, S. El-Marsafy, *Asia-Pac. J. Chem. Eng.* **2020**, *15 (3)*, e2460. DOI: https://doi.org/10.1002/apj.2460

[35] C. Costa, M. Demartini, R. Di Felice, M. Oliva, P. Pagliai, *Can. J. Chem. Eng.* **2019**, *97 (5)*, 1160–1171. DOI: https://doi.org/10.1002/cjce.23320

[36] C. Costa, R. Di Felice, P. Moretti, M. Oliva, R. Ramezani, *Can. J. Chem. Eng.* **2020**, *98 (12)*, 2516–2529. DOI: https://doi.org/10.1002/cjce.23820

[37] C. Kale, A. Górak, H. Schoenmakers, *Int. J. Greenhouse Gas Control* **2013**, *17*, 294–308. DOI: https://doi.org/10.1016/j.ijggc.2013.05.019

[38] H. M. Kvamsdal, J. P. Jakobsen, K. A. Hoff, *Chem. Eng. Process.* **2009**, *48 (1)*, 135–144. DOI: https://doi.org/10.1016/j.cep.2008.03.002

[39] P. Valeh-e-Sheyda, H. Rashidi, F. Ghaderzadeh, *J. Therm. Anal. Calorim.* **2019**, *135 (3)*, 1899–1909. DOI: https://doi.org/10.1007/s10973-018-7215-x

[40] Y. Haroun, L. Raynal, *Oil Gas Sci. Technol.* **2016**, *71 (3)*, 43. DOI: https://doi.org/10.2516/ogst/2015027

[41] M. Haghshenas Fard, M. Zivdar, R. Rahimi, M. Nasr Esfahani, A. Afacan, K. Nandakumar, K. Chuang, *Chem. Eng. Technol.* **2007**, *30 (7)*, 854–861. DOI: https://doi.org/10.1002/ceat.200700011

[42] S. H. Hosseini, S. Shojaee, G. Ahmadi, M. Zivdar, *J. Ind. Eng. Chem.* **2012**, *18 (4)*, 1465–1473. DOI: https://doi.org/10.1016/j.jiec.2012.02.012

[43] M. Isoz, in *Proc. Topical Problems of Fluid Mechanics*, Institute of Thermomechanics AS CR, PRague **2017**, 171–184. DOI: https://doi.org/10.14311/TPFM.2017.023

[44] M. K. Nikou, M. Ehsani, *Int. Commun. Heat Mass Transfer* **2008**, *35 (9)*, 1211–1219. DOI: https://doi.org/10.1016/j.icheatmasstransfer.2008.05.017

[45] B. Szulczewska, I. Zbicinski, A. Gorak, *Chem. Eng. Technol.* **2003**, *26 (5)*, 580–584. DOI: https://doi.org/10.1002/ceat.200390089

[46] D. Yu, D. Cao, Z. Li, Q. Li, *Chem. Eng. Res. Des.* **2018**, *129*, 170–181. DOI: https://doi.org/10.1016/j.cherd.2017.10.035

[47] M. Mazarei Sotoodeh, M. Zivdar, R. Rahimi, *J. Chem. Pet. Eng.* **2017**, *51 (1)*, 27–37. DOI: https://doi.org/10.22059/JCHPE.2017.62163

[48] M. A. Hossain, S. A. Nabavi, P. Ranganathan, L. Könözsy, V. Manovic, *Chem. Eng. Sci.* **2020**, *225*, 115800. DOI: https://doi.org/10.1016/j.ces.2020.115800

[49] S. A. Aromada, L. Øi, in *Proc. of the 56th Conf. on Simulation and Modelling (SIMS 56)*, Linköping University Electronic Press, Linkköping **2015**, 21–29. DOI: https://doi.org/10.3384/ecp1511921

[50] S. Mudhasakul, H. m. Ku, P. L. Douglas, *Int. J. Greenhouse Gas Control* **2013**, *15*, 134–141. DOI: https://doi.org/10.1016/j.ijggc.2013.01.023

[51] Y. Lim, J. Kim, J. Jung, C. S. Lee, C. Han, *Energy Procedia* **2013**, *37*, 1855–1862. DOI: https://doi.org/10.1016/j.egypro.2013.06.065

[52] C. T. Molina, C. Bouallou, *Chem. Eng. J.* **2013**, *35*, 319–324. DOI: https://doi.org/10.3303/CET1335053

[53] B. A. Khan, A. Ullah, M. W. Saleem, A. N. Khan, M. Faiq, M. Haris, *Sustainability* **2020**, *12 (20)*, 8524. DOI: https://doi.org/10.3390/su12208524

[54] F. Li, A. Hemmati, H. Rashidi, *Process Saf. Environ. Prot.* **2020**, *142*, 83–91. DOI: https://doi.org/10.1016/j.psep.2020.06.006

[55] U. Brinkmann, A. Janzen, E. Y. Kenig, *Chem. Eng. J.* **2014**, *250*, 342–353. DOI: https://doi.org/10.1016/j.cej.2014.03.066

[56] I. Otaraku, F. Esemuze, *Am. J. Chem. Eng.* **2015**, *3 (2–1)*, 41–46. DOI: https://doi.org/10.11648/j.ajche.s.2015030201.15

[57] P. Faravar, Z. Zarei, M. G. Monjezi, *J. Environ. Chem. Eng.* **2020**, *8 (4)*, 103946. DOI: https://doi.org/10.1016/j.jece.2020.103946

[58] M. Rezakazemi, Z. Niazi, M. Mirfendereski, S. Shirazian, T. Mohammadi, A. Pak, *Chem. Eng. J.* **2011**, *168 (3)*, 1217–1226. DOI: https://doi.org/10.1016/j.cej.2011.02.019

[59] Z. Zhang, Y. Yan, L. Zhang, Y. Chen, S. Ju, *J. Nat. Gas Sci. Eng.* **2014**, *19*, 311–316. DOI: https://doi.org/10.1016/j.jngse.2014.05.023

[60] H. Arastoopour, J. Abbasian, *National Energy Technology Lab.(NETL), Albany, OR (United States).* **2014**. DOI: https://doi.org/10.2172/1253147

[61] D. Dariusz Asendrych, P. Niegodajew, S. Drobniak, *Chem. Process Eng.* **2013**, 269–282. DOI: https://doi.org/10.2478/cpe-2013-0022

[62] P. Niegodajew, D. Asendrych, *Appl. Math. Modell.* **2016**, *40 (23-24)*, 10222–10237. DOI: https://doi.org/10.1016/j.apm.2016.07.003

[63] D. A. Pham, Y. I. Lim, H. Jee, E. Ahn, Y. Jung, *Comput.-Aided Chem. Eng.* **2015**, *37*, 557–562. DOI: https://doi.org/10.1016/B978-0-444-63578-5.50088-8

[64] D. Q. Gbadago, H. T. Oh, D. H. Oh, C. H. Lee, M. Oh, *Int. J. Greenhouse Gas Control* **2020**, *95*, 102983. DOI: https://doi.org/10.1016/j.ijggc.2020.102983

[65] Y. Fu, J. Bao, R. K. Singh, R. F. Zheng, C. M. Anderson-Cook, K. S. Bhat, Z. Xu, *AIChE J.* **2022**, e17691. DOI: https://doi.org/10.1002/aic.17691

[66] H. Uwitonze, I. Lee, S. B. Suh, I. Lee, *Chem. Eng. Process.* **2021**, *165*, 108429. https://doi.org/10.1016/j.cep.2021.108429

[67] M. Isoz, J. Haidl, *Ind. Eng. Chem. Res.* **2018**, *57 (34)*, 11785–11796. DOI: https://doi.org/10.1021/acs.iecr.8b00676

[68] B. Sun, T. Bhatelia, R. P. Utikar, G. M. Evans, V. K. Pareek, *Chem. Eng. Res. Des.* **2021**, *167*, 318–326. DOI: https://doi.org/10.1016/j.cherd.2021.01.003

[69] J. Xue, Q. Li, J. Qi, Q. Wu, H. Zhao, L. Zhang, *Chem. Eng. Sci.* **2021**, *230*, 116179. DOI: https://doi.org/10.1016/j.ces.2020.116179

[70] A. Hassanvand, S. H. Esmaeili-Faraj, M. S. Moghaddam, R. Moradi, *Chem. Eng. Technol.* **2021**, *44 (1)*, 156–163. DOI: https://doi.org/10.1002/ceat.202000237

[71] T. D. Manh, N. D. Nam, H. Babazadeh, R. Moradi, *Chem. Eng. Technol.* **2020**, *43 (9)*, 1690–1698. DOI: https://doi.org/10.1002/ceat.202000060

[72] O. M. Basha, R. Wang, I. K. Gamwo, N. S. Siefert, B. I. Morsi, *Int. J. Chem. React. Eng.* **2020**, *18 (3)*, 20190207. DOI: https://doi.org/10.1515/ijcre-2019-0207

[73] B. Kawas, B. Mizzi, D. Rouzineau, M. Meyer, *Chem. Eng. Res. Des.* **2021**, *172*, 21–33. DOI: https://doi.org/10.1016/j.cherd.2021.05.027

[74] Y. Amini, J. Karimi-Sabet, M. Nasr Esfahany, M. Haghshenasfard, A. Dastbaz, *Sep. Sci. Technol.* **2019**, *54 (16)*, 2706–2717. DOI: https://doi.org/10.1080/01496395.2018.1549076

[75] Y. Amini, M. M. Shadman, J. Karimi-Sabet, *Sep. Sci. Technol.* **2021**, *57*, 1900–1909. DOI: https://doi.org/10.1080/01496395.2021.2009513

[76] Y. Al-Maqaleh, N. D. M. Raimondi, D. F. Fletcher, D. Rouzineau, M. Meyer, *Chem. Eng. Process.* **2022**, *175*, 108912. DOI: https://doi.org/10.1016/j.cep.2022.108912
[77] J. L. Kang, S. H. Huang, S. S. Jang, *Processes* **2022**, *10 (7)*, 1276. DOI: https://doi.org/10.3390/pr10071276
[78] Y. Haroun, L. Raynal, D. Legendre, *Chem. Eng. Sci.* **2012**, *75*, 342–348. DOI: https://doi.org/10.1016/j.ces.2012.03.011
[79] D. Sebastia-Saez, S. Gu, P. Ranganathan, K. Papadikis, *Int. J. Greenhouse Gas Control* **2013**, *19*, 492–502. DOI: https://doi.org/10.1016/j.ijggc.2013.10.013
[80] J. L. Kang, Y. C. Ciou, D. Y. Lin, D. S. H. Wong, S. S. Jang, *Chem. Eng. Res. Des.* **2019**, *147*, 43–54. DOI: https://doi.org/10.1016/j.cherd.2019.04.037
[81] J. L. Kang, Y. C. Ciou, D. Y. Lin, C. H. Cheng, D. S. H. Wong, S. S. Jang, *Comput.-Aided Chem. Eng.* **2018**, *44*, 817–822. DOI: https://doi.org/10.1016/B978-0-444-64241-7.50131-2
[82] J. Cooke, *Modelling of reactive absorption in gas-liquid flows on structured packing*, Ph.D. Thesis, University of Southampton **2016**. http://eprints.soton.ac.uk/id/eprint/397079
[83] B. Dong, X. Yuan, K. Yu, *Chem. Eng. Res. Des.* **2017**, *124*, 238–251. DOI: https://doi.org/10.1016/j.cherd.2017.06.017
[84] L. Yang, F. Liu, K. Saito, K. Liu, *Energies* **2018**, *11 (11)*, 3103. DOI: https://doi.org/10.3390/en11113103
[85] R. K. Singh, J. E. Galvin, X. Sun, *Int. J. Greenhouse Gas Control* **2017**, *64*, 87–98. DOI: https://doi.org/10.1016/j.ijggc.2017.07.005
[86] R. K. Singh, J. E. Galvin, X. Sun, *Chem. Eng. J.* **2018**, *353*, 949–963. DOI: https://doi.org/10.1016/j.cej.2018.07.067
[87] R. K. Singh, C. Wang, Z. Xu, *Int. J. Greenhouse Gas Control* **2018**, *79*, 181–192. DOI: https://doi.org/10.1016/j.ijggc.2018.11.001
[88] R. K. Singh, J. Bao, C. Wang, Y. Fu, Z. Xu, *Chem. Eng. J.* **2020**, *398*, 125548. DOI: https://doi.org/10.1016/j.cej.2020.125548
[89] M. Fourati, V. Roig, L. Raynal, *Chem. Eng. Sci.* **2013**, *100*, 266–278. DOI: https://doi.org/10.1016/j.ces.2013.02.041
[90] I. Iliuta, C. Petre, F. Larachi, *Chem. Eng. Sci.* **2004**, *59 (4)*, 879–888. DOI: https://doi.org/10.1016/j.ces.2003.11.020
[91] K. Lappalainen, M. Manninen, V. Alopaeus, *Chem. Eng. Sci.* **2009**, *64 (2)*, 207–218. DOI: https://doi.org/10.1016/j.ces.2008.10.009
[92] F. ç. Larachi, C. F. Petre, I. Iliuta, B. Grandjean, *Chem. Eng. Process.* **2003**, *42 (7)*, 535–541. DOI: https://doi.org/10.1016/S0255-2701(02)00073-9
[93] C. F. Petre, F. Larachi, I. Iliuta, B. Grandjean, *Chem. Eng. Sci.* **2003**, *58 (1)*, 163–177. DOI: https://doi.org/10.1016/S0009-2509(02)00473-6
[94] C. Alvarez-Fuster, N. Midoux, A. Laurent, J. C. Charpentier, *Chem. Eng. Sci.* **1980**, *35 (8)*, 1717–1723. DOI: https://doi.org/10.1016/0009-2509(80)85006-8
[95] D. Barth, C. Tondre, J. J. Delpuech, *Chem. Eng. Sci.* **1984**, *39 (12)*, 1753–1757. DOI: https://doi.org/10.1016/0009-2509(84)80110-4
[96] P. Blauwhoff, G. Versteeg, W. P. M. Van Swaaij, *Chem. Eng. Sci.* **1983**, *38 (9)*, 1411–1429. DOI: https://doi.org/10.1016/0009-2509(83)80077-3
[97] T. L. Donaldson, Y. N. Nguyen, *Ind. Eng. Chem. Fundam.* **1980**, *19 (3)*, 260–266. DOI: https://doi.org/10.1021/i160075a005
[98] S. Laddha, P. Danckwerts, *Chem. Eng. Sci.* **1981**, *36 (3)*, 479–482. DOI: https://doi.org/10.1016/0009-2509(81)80135-2
[99] R. Littel, G. Versteeg, W. P. M. Van Swaaij, *Chem. Eng. Sci.* **1992**, *47 (8)*, 2027–2035. DOI: https://doi.org/10.1016/0009-2509(92)80319-8
[100] E. Sada, H. Kumazawa, Z. Han, H. Matsuyama, *AIChE J.* **1985**, *31 (8)*, 1297–1303. DOI: https://doi.org/10.1002/aic.690310808
[101] E. Sada, H. Kumazawa, Y. Osawa, M. Matsuura, Z. Han, *Chem. Eng. J.* **1986**, *33 (2)*, 87–95. DOI: https://doi.org/10.1016/0300-9467(86)80038-7
[102] G. Versteeg, M. Oyevaar, *Chem. Eng. Sci.* **1989**, *44 (5)*, 1264–1268. DOI: https://doi.org/10.1016/0009-2509(89)87026-5
[103] G. W. Xu, C. F. Zhang, S. J. Qin, B. C. Zhu, *Ind. Eng. Chem. Res.* **1995**, *34 (3)*, 874–880. DOI: https://doi.org/10.1021/ie00042a020
[104] M. Caplow, *J. Am. Chem. Soc.* **1968**, *90 (24)*, 6795–6803. DOI: https://doi.org/10.1021/ja01026a041
[105] P. Danckwerts, *Chem. Eng. Sci.* **1979**, *34 (4)*, 443–446. DOI: https://doi.org/10.1016/0009-2509(79)85087-3
[106] J. Gáspár, A. M. Cormoş, *Comput. Chem. Eng.* **2011**, *35 (10)*, 2044–2052. DOI: https://doi.org/10.1016/j.compchemeng.2010.10.001
[107] D. Barth, C. Tondre, J. J. Delpuech, *Int. J. Chem. Kinet.* **1986**, *18 (4)*, 445–457. DOI: https://doi.org/10.1002/kin.550180404
[108] D. Sebastia-Saez, S. Gu, P. Ranganathan, K. Papadikis, *Int. J. Greenhouse Gas Control* **2015**, *33*, 40–50. DOI: https://doi.org/10.1016/j.ijggc.2015.08.016
[109] J. Gabrielsen, M. L. Michelsen, E. H. Stenby, G. M. Kontogeorgis, *AIChE J.* **2006**, *52 (10)*, 3443–3451. DOI: https://doi.org/10.1002/aic.10963
[110] W. L. McCabe, J. C. Smith, P. Harriott, *Unit operations of chemical engineering*, McGraw-Hill, New York **1993**.
[111] E. S. Hamborg, G. F. Versteeg, *Chem. Eng. J.* **2012**, *198*, 561–570. DOI: https://doi.org/10.1016/j.cej.2012.03.051
[112] A. Tunnat, P. Behr, K. Görner, *Energy Procedia* **2014**, *51*, 197–206. DOI: https://doi.org/10.1016/j.egypro.2014.07.023
[113] F. A. Tobiesen, H. F. Svendsen, O. Juliussen, *AIChE J.* **2007**, *53 (4)*, 846–865. DOI: https://doi.org/10.1002/aic.11133
[114] P. Suess, L. Spiegel, *Chem. Eng. Process* **1992**, *31 (2)*, 119–124. DOI: https://doi.org/10.1016/0255-2701(92)85005-M
[115] D. Cappelli, *Proceedings of CFD with OpenSource Software*, Nilsson. H. Chalmers University of Technology, Gothenburg, Sweden **2018**.
[116] X. Lu, P. Xie, D. Ingham, L. Ma, M. Pourkashanian, *Chem. Eng. Sci.* **2018**, *189*, 123–134. DOI: https://doi.org/10.1016/j.ces.2018.04.074
[117] J. Kim, D. A. Pham, Y. I. Lim, *Chem. Eng. Res. Des.* **2017**, *121*, 99–112. DOI: https://doi.org/10.1016/j.cherd.2017.03.008
[118] C. Jiangbo, L. Chunjiang, Y. Xigang, Y. Guocong, *Chin. J. Chem. Eng.* **2009**, *17 (3)*, 381–388. DOI: https://doi.org/10.1016/S1004-9541(08)60220-7
[119] J. Huang, M. Li, Z. Sun, M. Gong, J. Wu, *Ind. Eng. Chem. Res.* **2015**, *54 (17)*, 4871–4878. DOI: https://doi.org/10.1021/ie504689s

[120] A. Lautenschleger, A. Olenberg, E. Kenig, *Chem. Eng. Sci.* **2015**, *122*, 452–464. DOI: https://doi.org/10.1016/j.ces.2014.09.040

[121] E. Karbasi, J. Karimi-Sabet, J. Mohammadi-Rovshandeh, M. A. Moosavian, H. Ahadi, Y. Amini, *Chem. Eng. J.* **2017**, *322*, 667–678. DOI: https://doi.org/10.1016/j.cej.2017.03.031

[122] P. F. Jahromi, J. Karimi-Sabet, Y. Amini, H. Fadaei, *Chem. Eng. J.* **2017**, *328*, 1075–1086. DOI: https://doi.org/10.1016/j.cej.2017.07.096

[123] M. Lungu, H. Wang, G. Mwandila, J. Wang, Y. Yang, F. Chen, J. Siame, *Powder Technol.* **2018**, *336*, 594–608. DOI: https://doi.org/10.1016/j.powtec.2018.06.028

[124] H. Wang, M. Lungu, Z. Huang, J. Wang, Y. Yang, Y. Yang, *Adv. Powder Technol.* **2018**, *29 (7)*, 1617–1631. DOI: https://doi.org/10.1016/j.apt.2018.03.026

[125] X. Lu, P. Xie, D. Ingham, L. Ma, M. Pourkashanian, *Chem. Eng. Sci.* **2019**, *199*, 302–318. DOI: https://doi.org/10.1016/j.ces.2019.01.029

[126] Y. Amini, M. Nasr Esfahany, *Sep. Sci. Technol.* **2019**, *54 (15)*, 2536–2554. DOI: https://doi.org/10.1080/01496395.2018.1549078

[127] S. I. Ngo, Y. I. Lim, *ChemEngineering* **2020**, *4 (2)*, 23. DOI: https://doi.org/10.3390/chemengineering4020023

[128] D. A. Pham, Y. I. Lim, H. Jee, E. Ahn, Y. Jung, *AIChE J.* **2015**, *61 (12)*, 4412–4425. DOI: https://doi.org/10.1002/aic.14962

[129] A. Zakeri, A. Einbu, P. O. Wiig, L. E. Øi, H. F. Svendsen, *Energy Procedia* **2011**, *4*, 606–613. DOI: https://doi.org/10.1016/j.egypro.2011.01.095

[130] Y. Amini, J. Karimi-Sabet, M. N. Esfahany, *Chem. Eng. Technol.* **2016**, *39 (6)*, 1161–1170. DOI: https://doi.org/10.1002/ceat.201500477

[131] J. Fernandes, P. C. Simões, J. P. Mota, E. Saatdjian, *J. Supercrit. Fluids.* **2008**, *47 (1)*, 17–24. DOI: https://doi.org/10.1016/j.supflu.2008.07.008

[132] W. Qi, K. Guo, H. Ding, D. Li, C. Liu, *Chem. Eng. Process.* **2017**, *118*, 62–70. DOI: https://doi.org/10.1016/j.cep.2017.04.020

[133] M. Tang, S. Zhang, D. Wang, Y. Liu, L. Wang, C. Liu, *Chem. Eng. Sci.* **2018**, *191*, 383–397. DOI: https://doi.org/10.1016/j.ces.2018.06.080

[134] M. Qiao, S. Liu, W. Huang, R. Hao, T. Zhang, S. Wu, *Can. J. Chem. Eng.* **2020**, *98 (10)*, 2238–2256. DOI: https://doi.org/10.1002/cjce.23751

[135] J. R. Hendry, J. G. Lee, P. S. Attidekou, *Chem. Eng. Process.* **2020**, *151*, 107908. DOI: https://doi.org/10.1016/j.cep.2020.107908

[136] P. Alix, L. Raynal, *Chem. Eng. Res. Des.* **2008**, *86 (6)*, 585–591. DOI: https://doi.org/10.1016/j.cherd.2008.02.021

[137] M. Fourati, V. Roig, L. Raynal, *Chem. Eng. Sci.* **2012**, *80*, 1–15. DOI: https://doi.org/10.1016/j.ces.2012.05.031

[138] J. Mackowiak, *Fluid Dynamics of Packed Columns*, Springer, Berlin **2010**. DOI: https://doi.org/10.1007/b98397

[139] Ž. Olujić, A. Kamerbeek, J. De Graauw, *Chem. Eng. Process.* **1999**, *38 (4–6)*, 683–695. DOI: https://doi.org/10.1016/S0255-2701(99)00068-9

[140] L. H. Macfarlan, M. T. Phan, R. B. Eldridge, *Chem. Eng. Sci.* **2022**, *249*, 117353. DOI: https://doi.org/10.1016/j.ces.2021.117353

[141] V. Bessou, D. Rouzineau, M. Prevost, F. Abbé, C. Dumont, J. P. Maumus, M. Meyer, *Chem. Eng. Sci.* **2010**, *65 (16)*, 4855–4865. DOI: https://doi.org/10.1016/j.ces.2010.05.029

[142] D. Dariusz Asendrych, P. Niegodajew, S. Drobniak, *Chem. Process Eng.* **2013**, *34 (2)*, 269–282. DOI: https://doi.org/10.2478/cpe-2013-0022

[143] L. Valenz, J. Haidl, V. Linek, *Ind. Eng. Chem. Res.* **2013**, *52 (17)*, 5967–5974. DOI: https://doi.org/10.1021/ie302397q

[144] L. H. Macfarlan, M. T. Phan, R. B. Eldridge, *Chem. Eng. Process.* **2022**, *172*, 108798. DOI: https://doi.org/10.1016/j.cep.2022.108798

[145] F. Chu, L. Yang, X. Du, Y. Yang, *Energy* **2016**, *109*, 495–505. DOI: https://doi.org/10.1016/j.energy.2016.04.123

[146] F. Chu, G. Xiao, G. Yang, *Sustainable Energy Fuels* **2021**, *5 (2)*, 438–448. DOI: https://doi.org/10.1039/D0SE01251C

[147] K. Fu, W. Rongwong, Z. Liang, Y. Na, R. Idem, P. Tontiwachwuthikul, *Chem. Eng. J.* **2015**, *260*, 11–19. DOI: https://doi.org/10.1016/j.cej.2014.08.064

[148] Y. Yu, T. Zhang, G. Liu, Z. Zhang, G. Wang, *Int. J. Heat Mass Transfer* **2017**, *144*, 501–516. DOI: https://doi.org/10.1016/j.ijheatmasstransfer.2017.06.048

[149] B. Xu, H. Gao, X. Luo, H. Liao, Z. Liang, *Int. J. Greenhouse Gas Control* **2016**, *51*, 11–17. DOI: https://doi.org/10.1016/j.ijggc.2016.05.004